Toward understanding the growth mechanism of Aun(SR)m nanoclusters: Effect of solvent on cluster size.

ARTICLE *in* RSC ADVANCES · MAY 2013

Impact Factor: 3.84

1 AUTHOR:

Gao Li

Dalian Institute of Chemical Physics

47 PUBLICATIONS **1,214** CITATIONS

SEE PROFILE

RSC Advances

RSC Publishing

PAPER

View Article Online
View Journal | View Issue

Cite this: *RSC Advances*, 2013, **3**, 9778

Toward understanding the growth mechanism of $Au_n(SR)_m$ nanoclusters: effect of solvent on cluster size

Chao Liu,[ab] Gao Li,[b] Guangsheng Pang*[a] and Rongchao Jin*[b]

Received 13th February 2013,
Accepted 22nd April 2013

DOI: 10.1039/c3ra40775f

www.rsc.org/advances

Despite the recent advances in size-controlled synthesis of thiolate-protected $Au_n(SR)_m$ nanoclusters, understanding the growth mechanism of nanoclusters still significantly lags behind. In this work, we report an important finding that the reaction medium plays a major role in influencing the final cluster size. Specifically, we focus on the one-phase synthetic process that leads to predominant formation of $Au_{25}(SR)_{18}$ or $Au_{144}(SR)_{60}$—two ubiquitous nanoclusters in nanocluster synthesis. When THF, acetone or ethyl acetate was used as the reaction solvent, we found that Au_{25} was formed as the major product, while in methanol or acetonitrile, predominant Au_{144} and some larger nanoparticles were formed. We mapped out some details of the underlying growth mechanism of nanoclusters, in which the reaction medium was found to affect the Au(I) intermediate (*i.e.* size and aggregation state), which subsequently affects the final size of gold nanoclusters. The obtained insight into the growth of nanoclusters is expected to contribute to the development of new synthetic strategies.

Introduction

Gold nanoclusters have received wide interest owing to their elegant optical properties,[1,2] catalytic promise,[3–5] and many other applications. Relatively large gold nanoparticles with size above ~2 nm (or equivalently above ~300 atoms) possess face-centered cubic (*fcc*) structure and exhibit surface plasma resonance (SPR).[6] On the other hand, ultra-small Au nanoparticles with size smaller than ~2 nm often adopt non-fcc structures, and significant quantization behavior occurs due to ultra-small size.[1,2,7–10] These ultra-small particles are often called nanoclusters in order to differentiate them from the conventional plasmonic nanoparticles.

Metal nanoclusters with quantum confinement effect are very sensitive to size, thus, controlling nanoclusters with atomic precision is very critical in both synthesis and studies of their unique properties.[1,7–16] In terms of the number of metal atoms in quantum nanoclusters, the range of ~10 to ~300 is particularly important,[1] because over this range the evolution from quantum behavior to classical metallic state will occur.[6–8] Recently, major advances have been attained in synthesizing *atomically precise* nanoclusters, and a number of size-discrete gold nanoclusters have been synthesized in pure form, such as $Au_{20}(SR)_{16}$,[17] $Au_{24}(SR)_{20}$,[18] $Au_{25}(SR)_{18}$,[19–22] $Au_{36}(SR)_{24}$,[23] $Au_{38}(SR)_{24}$,[24,25] $Au_{40}(SR)_{24}$,[26,27] $Au_{55}(SR)_{31}$,[28,29] $Au_{67}(SR)_{35}$,[30] $Au_{102}(SR)_{44}$,[31] $Au_{130}(SR)_{50}$,[32] $Au_{144}(SR)_{60}$,[33] *etc.* (where, SR represents thiolate generally).

With respect to the synthetic control of nanoclusters and mechanistic understanding, we have developed a successful size-focusing methodology,[34] which has been demonstrated to quite universal, and many of the aforementioned nanoclusters can be obtained in molecular purity by this method. The size focusing method consists of two primary steps, i) the synthesis of a crude product with a *controlled* size range, ii) size focusing of these clusters into a single-size product under harsh conditions. A critical step in this method is to precisely control the size range of the crude product in the first step,[34–36] otherwise two or more stable sizes would be resulted in the second step, and separation of them are difficult. On the other hand, despite the development of the size-focusing synthesis[6,30,32–37] and other methods such as gel or chromatographic separation[7,11,26,27,38] as well as size conversion,[23,38–40] understanding the growth mechanism of nanoclusters is still largely lagged behind, in particular what factors affect the size of the cluster product?

Herein we are motivated to gain some insight into the growth mechanism of nanoclusters. In this work, we have identified that the reaction medium (*i.e.* solvent) indeed has some unexpected, major influences on the final product size. The solvent effect can be correlated with the Au(I)-SR intermediate formation, and the aggregation state of Au(I)-SR should be one of the critical factors that control the final product size. Such insight is meaningful and important for understanding the nanocluster growth mechanism and for better control over cluster size in synthesis.

[a]*State Key Laboratory of Inorganic Synthesis and Preparative Chemistry, Jilin University, 2699 Qianjin Street, Changchun, Jilin 130012, China. E-mail: panggs@jlu.edu.cn*

[b]*Department of Chemistry, Carnegie Mellon University, 4400 Fifth Ave, Pittsburgh, PA 15213, USA. E-mail: rongchao@andrew.cmu.edu*

Experimental

Chemicals

All chemicals are commercially available and were used as received. Tetraoctylammonium bromide (TOAB, >98%) was purchased from Fluka. Tetrachloroauric(III) acid trihydrate ($HAuCl_4 \cdot 3H_2O$), sodium borohydride ($NaBH_4$, 99.99%), tetrahydrofuran (THF, HPLC grade, 99.9%), methanol (HPLC grade, 99.9%), dichloromethane (HPLC grade, 99.9%), acetone (HPLC grade, 99%), acetonitrile (HPLC grade, 99%), and ethyl acetate (HPLC grade, 99%) were obtained from Sigma-Aldrich. 2-phenylethanethiol (PhC_2H_4SH, 96%) and 1-hexanethiol ($C_6H_{13}SH$) were purchased from Acros Organics.

Synthesis of gold nanoclusters

As reported earlier,[35,41] we adopted a one-phase method to prepare gold nanoclusters using different solvents (see Results and Discussion), with other reaction conditions kept the same as reported). Typically, $HAuCl_4 \cdot 3H_2O$ (0.2 mmol) and TOAB (0.232 mmol) were add to a 50 ml tri-neck round-bottom flask, and then 15 ml of each of the chosen solvents was added. The solution turned red brown after stirring for ~20 min. Then, 2-phenylethanethiol or $C_6H_{13}SH$ (thiol/Au ratio: 5/1) was added to the solution, and the mixture was stirred for 30 mins or more until the red brown solution faded out, indicating reduction of $[Au(III)X_4]^-TOA^+$ (X = Cl/Br, TOA = tetraoctylammonium) into Au(I)SR, at which we observed, depending on the solvent use, either a nearly clear solution or a suspension with lots of white precipitates. A fresh aqueous $NaBH_4$ solution (6 ml, ice cold, $NaBH_4$/Au molar ratio: 10/1) was added to further reduce Au(I)SR into clusters. The reaction was allowed to proceed for 4 h. The black precipitate was washed with methanol for 4 times; then gold nanoclusters were extracted with CH_2Cl_2 and the extraction was repeated three times.

Characterization

MALDI mass spectrometry was performed on a PerSeptive Biosystems Voyager DE super-STR time-of–flight (TOF) mass spectrometer. *Trans*-2-[3-(4-*tert*-butylphenyl)-2-methy-2-propenyldidene] malonitrile (DCTB) was used as the matrix.[42] UV-vis spectra of the nanoclusters were recorded on a Hewlett-Packard (HP) Agilent 8453 diode array spectrophotometer at room temperature. Transmission electron microscopy (TEM) imaging was performed on a Hitachi H7500 electron microscope (acceleration voltage: 75 kV). The Au(I)SR solution (or suspension) was directly spotted onto a carbon film TEM grid. After solvent evaporation (in air), the grid was imaged under TEM.

Result and discussion

The $Au_{25}(SR)_{18}$ and $Au_{144}(SR)_{60}$ nanoclusters are quite ubiquitous in many synthetic experiments, indicating their facile formation in solution. Both Au_{25} and Au_{144} have been synthesized with SCH_2CH_2Ph, long chain SC_nH_{2n+1}, and many other types of aqueous and organic soluble thiolates.[19–22,41–43] The ligand independency indicates the robustness of the Au_{25} and Au_{144} atomic packing structures. The crystal structure of $Au_{25}(SCH_2CH_2Ph)_{18}$ has been determined[1,2]—which comprises a Au_{13} core and a protecting $Au_{12}(SR)_{18}$ shell, the latter can be viewed as six $Au_2(SR)_3$ dimeric staple motifs.[2] Crystallization of $Au_{144}(SCH_2CH_2Ph)_{60}$ has not been successful yet.[1] The Au_{25} nanocluster has been extensively studied, including its electronic structure and optical properties,[44–48] as well as the ligand-exchange behavior.[49] Three distinct absorption bands were observed at 400, 450 and 670 nm for Au_{25}, which were also reproduced in DFT simulations[44] and thus their origins of electronic transitions have been interpreted. Au_{144} also show absorption bands at 510 and 700 nm,[24,33] though not as pronounced as those bands of Au_{25}. These optical features conveniently serve as spectroscopic 'fingerprints' for preliminary identification of cluster size in a crude product.

With respect to the synthesis, Au_{25} can be prepared in high yield and molecular purity by the two-phase or one-phase method.[21,35] In our efforts to make larger nanoclusters (*e.g.* Au_{144}) with the one-phase method,[41] we found that Au_{25} tends to be present as a by-product but can be separated by solvent extraction.[41] Therefore, it would be interesting and meaningful to find out what factor(s) determine the respective formation of Au_{25} and Au_{144} clusters. We speculate that there could be some relationship between the reaction solvent and size controllability of gold nanoclusters. Herein we employ the one-phase method[41] to carry out a systematic study of the solvent effect.

We chose five common solvents in this work, including THF, acetone, ethyl acetate, methanol and acetonitrile. Starting with $HAuCl_4 \cdot 3H_2O$, the primary reactions include i) the reduction of Au(III) into Au(I)-SR by excess thiol, ii) aggregation of Au(I)-SR monomers into oligomeric or polymeric $[Au(I)SR]_x$, iii) further reduction of Au(I) into polydisperse clusters, and iv) size focusing into one specific size (or at least one predominant size) in the final product.

Our results show that when THF, acetone and ethyl acetate were respectively used as the solvent in the one-phase synthesis experiments (see Experimental for details), the major product is Au_{25} clusters, evidenced by the optical absorption spectra of the crude products, which show absorption peaks at 450 and 670 nm (Fig. 1A, profiles a–c), consistent with those peaks of pure Au_{25} clusters (Fig. 1A, profile d). Of note, in the case of acetone as the reaction medium, we observed another two near-IR peaks at 820 and 1050 nm (Fig. 1A, profile c). We have not been able to identify what species these optical peaks belong to. Meng *et al.*[50] reported that the optical spectrum with a peak at 820 nm should be associated with gold nanoclusters of Au_{39} and Au_{40}. Efforts are still necessary to determine the exact size of the near-IR species in the present case.

We further employ MALDI-TOF to characterize the above crude products and to identify the cluster size(s). The positive mode mass spectra (Fig. 1B) show that Au_{25} (mass of intact $Au_{25}(SC_2H_4Ph)_{18}$ cluster ion: 7394 Da, charge +1) is indeed the predominant product for all the three solvents, consistent with

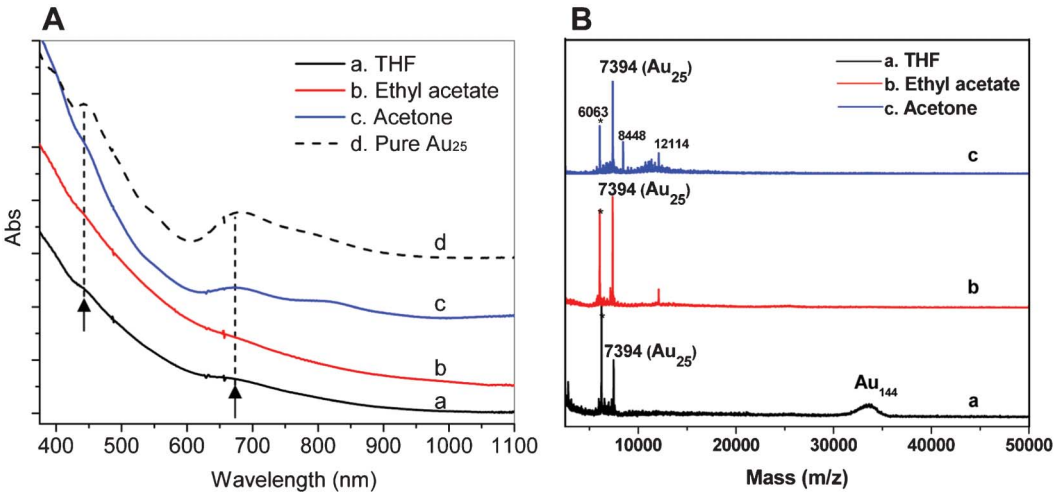

Fig. 1 (A) Optical absorption spectra (a–c) of products obtained in acetone, ethyl acetate and THF, respectively, and (d) spectrum of pure $Au_{25}(SCH_2CH_2Ph)_{18}^{-}TOA^{+}$, (B) MALDI mass spectra of products obtained in acetone, ethyl acetate and THF, respectively.

the observed optical spectral features (Fig. 1A); note that the mass peak at ~6063 is a known fragment of $Au_{25}(SR)_{18}$ (assigned to $Au_{21}(SR)_{14}$, due to loss of $Au_4(SR)_4$).[42,51] Compared to the spectrum of pure Au_{25}, the less prominent peaks of the crude products indicate that some impurity (*e.g.* unreduced Au(I)SR complexes and possibly other species) exists in the crude product, albeit the predominant product is Au_{25}. We indeed found a small amount of Au_{144} clusters in the case of THF as the solvent (Fig. 1B, profile a), but the mass spectra for the ethyl acetate and acetone cases showed no Au_{144}. The Au_{144} clusters can be removed by acetone extraction (note: smaller clusters dissolve in acetone while Au_{144} doesn't).[41] In the cases of acetone and ethyl acetate as solvents, beside the predominant Au_{25} cluster, another gold nanocluster was observed at 12 114 Da, which is tentatively assigned to Au_{42}, but the abundance was not high. After extraction with acetone (note: not to be confused with *acetone* as the reaction solvent), the acetone-insoluble Au_{42} nanocluster was removed and the acetone soluble product consists of highly pure Au_{25} clusters (Fig. 2). The optical spectra of the crude product (before acetone extraction) and acetone-insoluble and soluble components are compared in Fig. 2; apparently, the acetone-soluble species is pure Au_{25}, judging by the optical spectrum, while the acetone-insoluble species is attributed to Au_{42} which shows absorption bands at 820 and 1050 nm.

Taken together, the MALDI-TOF and optical spectroscopic data both confirm that Au_{25} is the major product for the three investigated solvents—THF, acetone and ethyl acetate. Interestingly, we found another category of solvents, such as methanol and acetonitrile, which favor the predominant formation of Au_{144}, instead of Au_{25}. Herein, we followed the same one-phase synthetic method for a close comparison with the above experiments that lead to Au_{25}.

When methanol was used as the solvent, the optical absorption spectrum shows very weak bands at ~510 and 710 nm—which are attributed to Au_{144} (Fig. 3A, spectrum b); note that the absorption peaks of Au_{144} are inherently less prominent than those of Au_{25}, hence spectroscopic identification of Au_{144} is not as easy as the identification of Au_{25}. When CH_3CN was used as the solvent, the optical spectrum exhibits a surface plasmon resonance (SPR) peak at ~520 nm, indicating the presence of large plasmonic nanoparticles (>2 nm) in the crude product (Fig. 3A, spectrum a). We then characterized the products by MALDI-MS. For acetonitrile as the solvent, the MALDI-TOF spectrum shows a broad peak from 31–36 kDa and some Au_{25} clusters as well (Fig. 3B, profile a). When methanol was used as the solvent, in addition to the ~30 kDa peak (major) some Au_{25} clusters also appeared. It is worth noting that different laser intensities were used in MALDI analysis and some ligands were inevitably lost from the clusters, giving rise to the peak shift of Au_{144} from ~34 kDa to

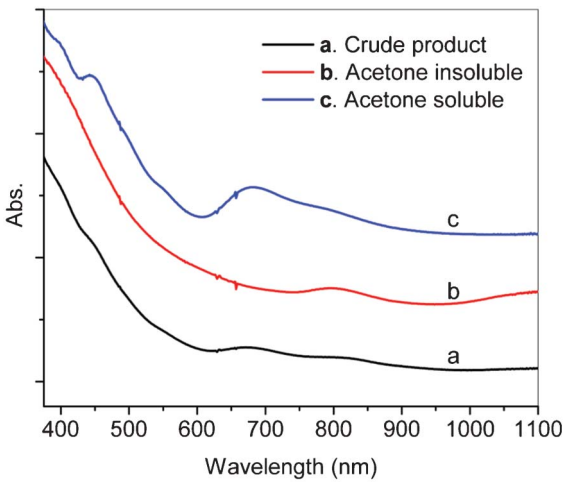

Fig. 2 The optical absorption spectra of crude product (profile a) obtained in acetone (as reaction medium) and nanoclusters of acetone-insoluble (profile b) and soluble (profile c).

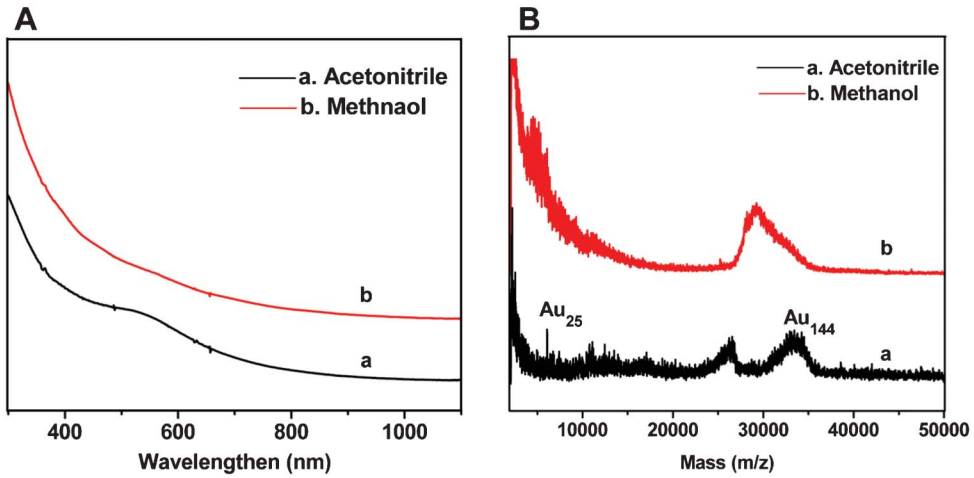

Fig. 3 (A) Optical absorption spectra and (B) MALDI-MS spectra of products prepared in acetonitrile and methanol (reaction medium), respectively.

~29 kDa depending on the laser intensity. The plasmonic nanoparticles in the case of acetonitrile were not identified in MALDI analysis. Overall, when methanol or acetonitrile was used as the solvent, Au_{144} clusters (and larger nanoparticles in acetonitrile) were the major products, while Au_{25} was minor.

The above results identified two classes of solvents for the respective formation of Au_{25} and Au_{144} clusters in the one-phase synthesis. To further test the generality of the distinct effect of solvent, we replaced 2-phenylethanethiol with 1-hexanethiol. Indeed, we found a similar solvent effect as afore-discussed for 2-phenylethanethiol, that is, Au_{25} was the major product when THF, ethyl acetate, or acetone was the solvent (Fig. 4A–C, black profiles), and in contrast, Au_{144} clusters were obtained in methanol or acetonitrile (Fig. 4D–E, black profiles). It should be noted that when using 1-hexanethiol as the ligand, no Au_{42} was observed in acetone (or

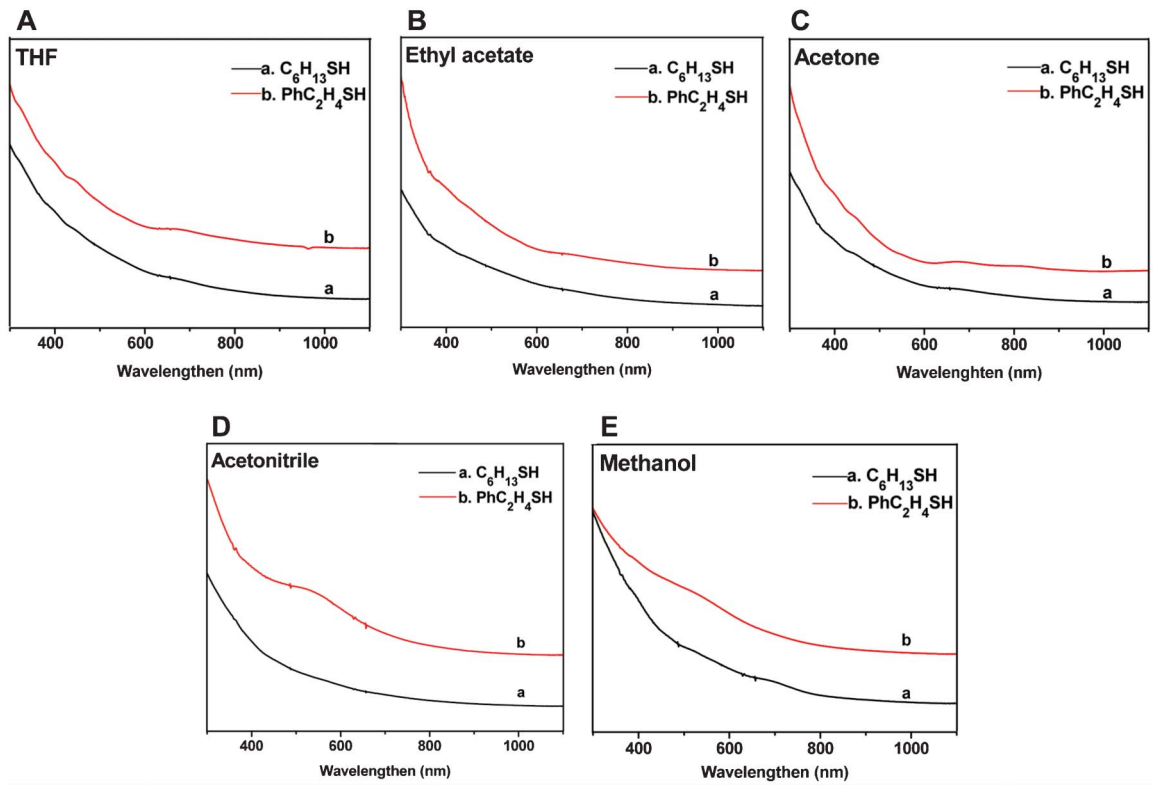

Fig. 4 Comparison of the optical absorption spectra of samples obtained with different ligands (PhC_2H_4SH (red) *versus* $C_6H_{13}SH$ (black)), each ligand was tested with five solvents in the synthesis.

ethyl acetate) as the reaction solvent; the optical absorption spectra indicate Au_{25} as the major product, while no other peaks were observed.

The above results clearly show that one category of solvents (*e.g.* acetone, ethyl acetate and THF) predominantly produces Au_{25}, while another category of solvents (*e.g.* acetonitrile and methanol) predominantly produces Au_{144} (Scheme 1). Herein we attempt to further correlate the respective growth of Au_{25} and Au_{144} nanoclusters with the Au(I)SR intermediates based upon experimental observations of the solvent effect and the Au(I)SR formation.

When the thiol (HS-C_2H_4Ph or HS-C_6H_{13}) was added to the THF, acetone, or ethyl acetate solution of Au(III) salt, the resultant Au(I)SR intermediate was a nearly colorless, transparent solution (Fig. 5A inset), implying *small* $[Au(I)SR]_x$ species from aggregation of Au(I)SR monomers. TEM imaging of the residuals of the solution (after solvent evaporation) showed small (*ca.* 100–200 nm), flake-like amorphous substances (Fig. 5A), and dynamic light scattering (DLS) confirmed the size range. In contrast, when the thiol was added to a methanol or acetonitrile solution of Au(III) salt, the Au(I)SR intermediate was visually observed to be a white precipitate (Fig. 5B inset), implying *large* $[Au(I)SR]_x$ aggregates (>100 μm human eye resolution), which are also seen in TEM imaging (Fig. 5B) and the aggregate sizes are of order $\sim 10^2$ μm. Such large aggregates in solution state could not be measured by DLS (detection range: up to 10 μm). We also performed a test: the white precipitate from MeCN or MeOH was transferred to THF (solvent), but we observed that the precipitate did not dissolve in THF, which indicates that once the aggregates are formed in MeCN or MeOH, they cannot be broken by THF solvation; thus, the size difference between the two categories of solvents is intrinsic, rather than due to *insolubility* in one solvent *versus* the other. Taken together, these observations indicate the dispersity of the Au(I)SR monomers is closely related to the solvent, which leads to the different sized $[Au(I)SR]_x$ aggregates. Unfortunately, the large $[Au(I)SR]_x$ polymeric species are not amenable for in depth characterization, thus detailed information still cannot be obtained at this stage. It is also noteworthy that $[Au(I)X_2]^-$ (where X = halide) may become the intermediate in the reaction system when no water was present.[52,53] Thus, the formation of Au(I) intermediates is quite complicated. Overall, by correlating the $[Au(I)SR]_x$ aggregate size with the optical spectroscopic and MALDI-MS analyses of the final cluster product, we mapped out that small $[Au(I)SR]_x$ favors Au_{25} formation, whereas large $[Au(I)SR]_x$ aggregates favor the formation of Au_{144}. Of note, Au_{38} formation needs a heating condition, as demonstrated in our recent work;[54] hence, the ubiquitous Au_{38} clusters were not observed in the present one-phase room temperature synthesis process.

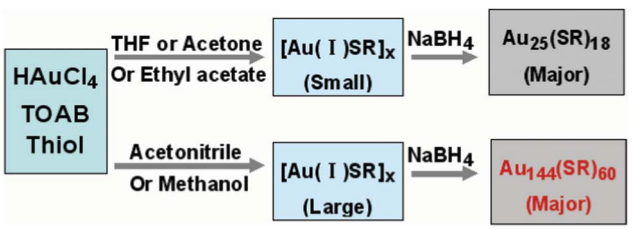

Scheme 1 Effect of solvent on cluster size of the product.

It is worth noting that previous work by Hainfeld and coworkers[55] utilized solution pH to control the size of polymeric Au(I):glutathione intermediates (25–150 nm, measured by DLS) for size control of gold nanoparticles ranging from 2 to 6 nm. Although our system is organic soluble and does not involve pH effect for size control of the Au(I) polymers, the essence in Hainfeld's work and our present work shares some interesting commons. For our organic system, the different sizes of Au(I) polymers in different solvents should be primarily due to the different *solvation* interactions which are balanced with Au(I)···Au(I) aurophilic interactions in the self-assembly process of Au(I):SR monomers into polymeric aggregates, as opposed to the pH-induced *electrostatic* repulsion in balance with aurophilic interactions in Hainfeld's work.

A rough picture for the growth of Au_{25} and Au_{144} clusters is as follow. In the first category of solvents, the relatively small $[Au(I)SR]_x$ should be readily reduced into (polydisperse) clusters upon the addition of $NaBH_4$. Since the $[Au(I)SR]_x$ size (of order $\sim 10^2$ nm) is much larger than the size of Au_{25} (1 nm), the aggregate must break into smaller pieces. With the second category of solvents, the resultant large $[Au(I)SR]_x$ aggregates (seen as white precipitate) were found to exhibit a slower rate in the conversion to clusters upon addition of $NaBH_4$, and these huge aggregates must first break down into much smaller pieces when reaction with $NaBH_4$. The slower reduction kinetics appears to result in larger clusters than the case of the first category of solvents. In both scenarios, the initially formed polydisperse clusters then undergo a size focusing process at room temperature. The Au_{25} clusters were predominantly formed when the size range of polydisperse clusters was controlled at the relatively low end ($\sim$5–8 kDa),[54] while Au_{144} was predominantly formed when the cluster size range was at the high end ($\sim$29–34 kDa).[33]

In additional to the factor of $[Au(I)SR]_x$ aggregates, other important parameters that influence the final cluster size may also include the solubility of nanoclusters in various solvents, and the functional group in the solvent molecule (such as the –CN group in acetonitrile) which seems to interact with gold cluster surface, evidenced by the less stability of $Au_{25}(SR)_{18}$ clusters in acetonitrile. To map out a more complete picture of the relationship between solvent and the final size of gold nanocluster still needs some further work. For future work, a major task is to probe the details of the Au(I)SR intermediate, include the structure and detailed morphology of $[Au(I)SR]_x$. It should be noted that, although the structure of $[Au(I)SR]_x$ polymer remains elusive, some Au(I) thiolate structures were indeed crystallographically characterized[56,57] and theoretically modeled.[58,59] The Au(I)SR polymers[56,60–62] likely exist in 2D extended sheets, lamellar structures, and/or random coils.

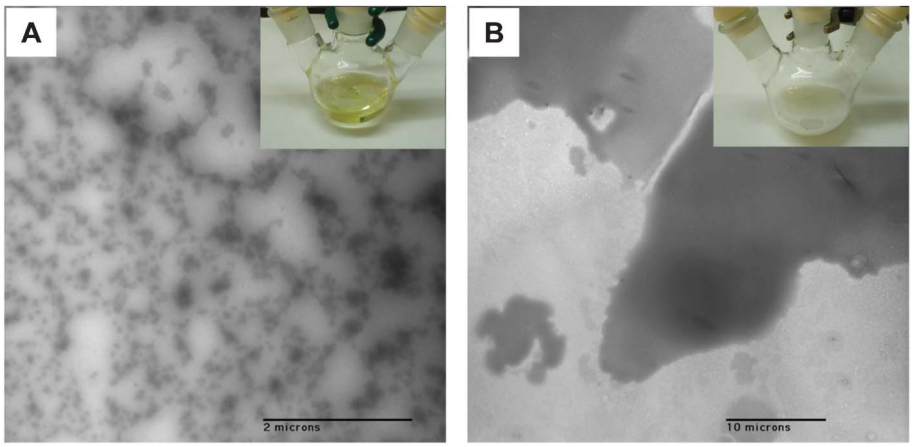

Fig. 5 TEM images and photographs (insets) of Au(I) intermediates in A) THF and B) methanol.

Indeed, extended sheet-like structures of Au(I) were observed by Odriozola *et al.*[62] In gold thiolate cluster synthesis, a $Au_4(SR)_4$ species was often observed.[63,64] In general, future work may elucidate more details on the correlation between the size/structure of $[Au(I)SR]_x$ and cluster growth.[65]

Conclusion

In summary, we have outlined the important effect of the reaction solvent on the final size of gold nanoclusters. When THF, acetone or ethyl acetate was used as the reaction solvent, Au_{25} was the major product, while with methanol or acetonitrile solvent predominant Au_{144} clusters were resulted, albeit some Au_{25} clusters or plasmonic nanoparticles were concurrently formed. The solvent effect should at least in part be related to the size and aggregation state of the Au(I):SR intermediate, which influences the final product size after reduction by $NaBH_4$. The identified relationship between the reaction solvent and the formation of different sized nanoclusters improves current understanding of nanocluster growth and will facilitate design of synthetic strategies for attaining size control of nanoclusters.

Acknowledgements

C. L. acknowledges the fellowship support by China Scholarship Council. S. P. acknowledges support by National Natural Science Foundation of China (#21071058). R. J. acknowledges support by the Air Force Office of Scientific Research under AFOSR Award No. FA9550-11-1-9999 (FA9550-11-1-0147).

References

1 H. Qian, M. Zhu, Z. Wu and R. Jin, *Acc. Chem. Res.*, 2012, **45**, 1470.
2 J. F. Parker, C. A. Fields-Zinna and R. W. Murray, *Acc. Chem. Res.*, 2010, **43**, 1289.
3 H. Tsunoyama, H. Sakurai, Y. Negishi and T. Tsukuda, *J. Am. Chem. Soc.*, 2005, **127**, 9374.
4 Y. Zhu, H. Qian, B. A. Drake and R. Jin, *Angew. Chem., Int. Ed.*, 2010, **49**, 1295.
5 M. Lee, P. Amaratunga, J. Kim and D. Lee, *J. Phys. Chem. C*, 2010, **114**, 18366.
6 H. Qian, Y. Zhu and R. Jin, *Proc. Natl. Acad. Sci. U. S. A.*, 2012, **109**, 696.
7 R. B. Wyrwas, M. M. Alvarez, J. T. Khoury, R. C. Price, T. G. Schaaff and R. L. Whetten, *Eur. Phys. J. D*, 2007, **43**, 91.
8 J.-i. Nishigaki, R. Tsunoyama, H. Tsunoyama, N. Ichikuni, S. Yamazoe, Y. Negishi, M. Ito, T. Matsuo, K. Tamao and T. Tsukuda, *J. Am. Chem. Soc.*, 2012, **134**, 14295.
9 E. S. Shibu and T. Pradeep, *Chem. Mater.*, 2011, **23**, 989.
10 P. R. Nimmala and A. Dass, *J. Am. Chem. Soc.*, 2011, **133**, 9175.
11 Y. Negishi, W. Kurashige, Y. Niihori, T. Iwasa and K. Nobusada, *Phys. Chem. Chem. Phys.*, 2010, **12**, 6219.
12 H. Qian, D.-e. Jiang, G. Li, C. Gayathri, A. Das, R. R. Gil and R. Jin, *J. Am. Chem. Soc.*, 2012, **134**, 16159.
13 S. Knoppe, R. Azoulay, A. Dass and T. Bürgi, *J. Am. Chem. Soc.*, 2012, **134**, 20302.
14 H. Yao, *J. Phys. Chem. Lett.*, 2012, **3**, 1701.
15 Y. Negishi, U. Kamimura, M. Ide and M. Hirayama, *Nanoscale*, 2012, **4**, 4263.
16 X. Yuan, Y. Yu, Q. Yao, Q. Zhang and J. Xie, *J. Phys. Chem. Lett.*, 2012, **3**, 2310.
17 M. Zhu, H. Qian and R. Jin, *J. Am. Chem. Soc.*, 2009, **131**, 7220.
18 M. Zhu, H. Qian and R. Jin, *J. Phys. Chem. Lett.*, 2010, **1**, 1003.
19 Y. Negishi, N. K. Chaki, Y. Shichibu, R. L. Whetten and T. Tsukuda, *J. Am. Chem. Soc.*, 2007, **129**, 11322.
20 J. B. Tracy, G. Kalyuzhny, M. C. Crowe, R. Balasubramanian, J.-P. Choi and R. W. Murray, *J. Am. Chem. Soc.*, 2007, **129**, 6706.
21 M. Zhu, E. Lanni, N. Garg, M. E. Bier and R. Jin, *J. Am. Chem. Soc.*, 2008, **130**, 1138.
22 A. C. Dharmaratne, T. Krick and A. Dass, *J. Am. Chem. Soc.*, 2009, **131**, 13604.

23 C. Zeng, H. Qian, T. Li, G. Li, N. L. Rosi, B. Yoon, R. N. Barnett, R. L. Whetten, U. Landman and R. Jin, *Angew. Chem., Int. Ed.*, 2012, **51**, 13114.
24 N. K. Chaki, Y. Negishi, H. Tsunoyama, Y. Shichibu and T. Tsukuda, *J. Am. Chem. Soc.*, 2008, **130**, 8608.
25 H. Qian, W. T. Eckenhoff, Y. Zhu, T. Pintauer and R. Jin, *J. Am. Chem. Soc.*, 2010, **132**, 8280.
26 H. Qian, Y. Zhu and R. Jin, *J. Am. Chem. Soc.*, 2010, **132**, 4583.
27 S. Knoppe, J. Boudon, I. Dolamic, A. Dass and T. Bürgi, *Anal. Chem.*, 2011, **83**, 5056.
28 H. Tsunoyama, Y. Negishi and T. Tsukuda, *J. Am. Chem. Soc.*, 2006, **128**, 6036.
29 H. Qian and R. Jin, *Chem. Commun.*, 2011, **47**, 11462.
30 P. R. Nimmala, B. Yoon, R. L. Whetten, U. Landman and A. Dass, *J. Phys. Chem. A*, 2013, **117**, 504.
31 Y. Levi-Kalisman, P. D. Jadzinsky, N. Kalisman, H. Tsunoyama, T. Tsukuda, D. A. Bushnell and R. D. Kornberg, *J. Am. Chem. Soc.*, 2011, **133**, 2976.
32 Y. Negishi, C. Sakamoto, T. Ohyama and T. Tsukuda, *J. Phys. Chem. Lett.*, 2012, **3**, 1624.
33 H. Qian and R. Jin, *Nano Lett.*, 2009, **9**, 4083.
34 R. Jin, H. Qian, Z. Wu, Y. Zhu, M. Zhu, A. Mohanty and N. Garg, *J. Phys. Chem. Lett.*, 2010, **1**, 2903.
35 Z. Wu, J. Suhan and R. Jin, *J. Mater. Chem.*, 2009, **19**, 622.
36 P. Maity, T. Wakabayashi, N. Ichikuni, H. Tsunoyama, S. Xie, M. Yamauchi and T. Tsukuda, *Chem. Commun.*, 2012, **48**, 6085.
37 V. L. Jimenez, D. G. Georganopoulou, R. J. White, A. S. Harper, A. J. Mills, D. Lee and R. W. Murray, *Langmuir*, 2004, **20**, 6864.
38 Y. Shichibu, Y. Negishi, T. Watanabe, N. K. Chaki, H. Kawaguchi and T. Tsukuda, *J. Phys. Chem. C*, 2007, **111**, 7845.
39 A. Das, T. Li, K. Nobusada, Q. Zeng, N. L. Rosi and R. Jin, *J. Am. Chem. Soc.*, 2012, **134**, 20286.
40 S. Park and D. Lee, *Langmuir*, 2012, **28**, 7049.
41 H. Qian and R. Jin, *Chem. Mater.*, 2011, **23**, 2209.
42 A. Dass, A. Stevenson, G. R. Dubay, J. B. Tracy and R. W. Murray, *J. Am. Chem. Soc.*, 2008, **130**, 5940.
43 Y. Shichibu, Y. Negishi, H. Tsunoyama, M. Kanehara, T. Teranishi and T. Tsukuda, *Small*, 2007, **3**, 835.
44 M. Zhu, C. M. Aikens, F. J. Hollander, G. C. Schatz and R. Jin, *J. Am. Chem. Soc.*, 2008, **130**, 5883.
45 P. Maity, S. Xie, M. Yamauchi and T. Tsukuda, *Nanoscale*, 2012, **4**, 4027.
46 G. A. Simms, J. D. Padmos and P. Zhang, *J. Chem. Phys.*, 2009, **131**, 214703.
47 S. Kumar and R. Jin, *Nanoscale*, 2012, **4**, 4222.
48 Y. Niihori, W. Kurashige, M. Matsuzaki and Y. Negishi, *Nanoscale*, 2013, **5**, 508.
49 X. Meng, Q. Xu, S. Wang and M. Zhu, *Nanoscale*, 2012, **4**, 4161.
50 X. Meng, Z. Liu, M. Zhu and R. Jin, *Nanoscale Res. Lett.*, 2012, **7**, 277.
51 Z. Wu, C. Gayathri, R. R. Gil and R. Jin, *J. Am. Chem. Soc.*, 2009, **131**, 6535.
52 Y. Li, O. Zaluzhna and Y. J. Tong, *Langmuir*, 2011, **27**, 7366.
53 Y. Li, O. Zaluzhna, C. D. Zangmeister, T. C. Allison and Y. J. Tong, *J. Am. Chem. Soc.*, 2012, **134**, 1990.
54 H. Qian, C. Liu and R. Jin, *Sci. China: Chem.*, 2012, **55**, 2359.
55 R. P. Briñas, M. Hu, L. Qian, E. S. Lymar and J. F. Hainfeld, *J. Am. Chem. Soc.*, 2008, **130**, 975.
56 I. G. Dance, K. J. Fisher, R. M. H. Banda and M. L. Scudder, *Inorg. Chem.*, 1991, **30**, 183.
57 C. F. Shaw, *Chem. Rev.*, 1999, **99**, 2589.
58 H. Grönbeck, M. Walter and H. Häkkinen, *J. Am. Chem. Soc.*, 2006, **128**, 10268.
59 N. Shao, Y. Pei, Y. Gao and X. C. Zeng, *J. Phys. Chem. A*, 2009, **113**, 629.
60 M. K. Corbierre and R. B. Lennox, *Chem. Mater.*, 2005, **17**, 5691.
61 F. Bensebaa, T. H. Ellis, E. Kruus, R. Voicu and Y. Zhou, *Langmuir*, 1998, **14**, 6579.
62 I. Odriozola, I. Loinaz, J. A. Pomposo and H. J. Grande, *J. Mater. Chem.*, 2007, **17**, 4843.
63 A. P. Gies, D. M. Hercules, A. E. Gerdon and D. E. Cliffel, *J. Am. Chem. Soc.*, 2007, **129**, 1095.
64 Z. Tang, B. Xu, B. Wu, M. W. Germann and G. Wang, *J. Am. Chem. Soc.*, 2010, **132**, 3367.
65 R. Jin, Y. Zhu and H. Qian, *Chem.–Eur. J.*, 2011, **17**, 6584.

